

Narendhran Sadhasivam\*

Department of Biotechnology, Sri Krishna Arts and Science College,  
Kuniamuthur, Coimbatore, India

Scientific paper

ISSN 0351-9465, E-ISSN 2466-2585

<https://doi.org/10.62638/ZasMat1131>



Zastita Materijala 65 (2)

246 - 257 (2024)

## Synergistic effect of Fe and Co doped ZnO nanoparticles synthesized using *Alpinia galanga* against *Candida parasilopsis*

### ABSTRACT

In this investigation, nanoparticles such as ZnO, Fe doped ZnO and Co doped ZnO NPs prepared by the co-precipitation method were tested against the pathogenic yeast. The spectroscopic analyses were carried out to identify the morphological and chemical composition of the synthesized nanoparticles. The results of XRD analysis revealed that the synthesized nanoparticles were crystalline in nature with average size ranges between 32 – 34 nm approximately. EDX and SEM analysis were carried out to identify the element composition (Co, Fe and Zn) and spherical shape of nanoparticles. The functional group that is responsible for the capping and stability of nanoparticles was confirmed by FTIR analysis, to compare the antifungal efficiency of ZnO, Fe doped ZnO and Co doped ZnO from the resultant zone of inhibition.

**Keywords:** Antifungal activity, *Candida parapsilosis*, Copper, Iron, Zinc

### 1. INTRODUCTION

Fungal infections are concerned to be a serious case of health conditions. The severity of the infections seems to be higher in the case of immune compromised people as they are more susceptible which in turn impairs their disease conditions. The administration of drugs resulting from modern medical inventions potentially have immune suppressive actions which is also considered to be one of the causes of high incidence of fungal infections. It is high time for the world to get cautious about fungal infections [1]. *Candida* species are opportunistic fungal pathogens in which both *Candida albicans* and non albicans candida species (eg, *Candida parapsilopsis*) have caused increased incidence of diseases recently. The severity of the infections is complex due to its associated virulence factors and the emergence of drug resistant strains. In such cases, a direct administration of such antifungal agents has many limitations such as toxicities, drug resistance etc [2]. The unavailability of many antifungal drugs as well as cost expenses limits its usage in many of the developing countries. Hence science and technology for developing a novel medication that will be affordable as well as effective in invading fungal diseases [3].

Over the last two decades, nanotechnology has been in high demand which changed the conventional drug administration processes. It is possible to have a targeted drug delivery as it emphasizes on submicron size particles in which mono or poly therapeutic compounds may either dispersed, adsorbed, covalently bonded, or encapsulated in vesicles, capsules, or polymeric matrix. Furthermore, the nanodrug delivery system enhances the bioavailability and decreases the possible side effects of the drug. Considering the wider perspective of nanotechnology in medicine, several researchers are making an exceptional effort to raise the standards of nano drugs by putting forward various methodologies to fabricate novel nano drug formulations [4]. Now-a days, metallic nanoparticles have gained immense attention as antimicrobial agents due to their high surface area to volume ratio, availability and ease of synthesis. Interestingly, green synthesis of nanoparticles from plant extracts is a striking area of research in nanotechnology. It is economically feasible and eco-friendly compared to physical and chemical routes [5].

*Alpinia galanga* is a plant belonging to zingiberacea family and is widely distributed in South East Asia. It has a role as a traditional medicine to cure inflammation, HIV, diabetes and ulcers. The *Alpinia galanga* leaf extracts contain pharmacologically significant metabolites such as galanolactones, quercetin, galangin, kaempferol, and labdane [6]. Consequently, due to their diverse pharmacological activities, these extracts could be extensively utilized in the synthesis of ZnO

\*Corresponding author: Sadhasivam Narendhran

Email: narendhrans@skasc.ac.in

Paper received: 27. 09. 2023.

Paper accepted: 09. 12. 2023.

Paper is available on the website: [www.idk.org.rs/journal](http://www.idk.org.rs/journal)

nanoparticles. Generally, metal and metal oxide nanoparticles have more application due to their stability when compared to other organic materials. ZnO have a very attractive attributes such as selective toxicity targeting prokaryotic cells, anticancer activities etc. They trigger mechanisms like apoptosis, necrosis, and the generation of reactive oxygen species (ROS) in their effects. Studies indicate that ZnO has proven to be a potent antibacterial agent, capable of selectively damaging membrane structures and compromising their integrity. Additionally, these nanoparticles can efficiently penetrate intracellular of bacteria, leading to damage to both DNA and proteins [5]. Usually ZnO is a chemically stable and biocompatible material with optical, electronic and magnetic properties.

Formulation of doped nanoparticles is another advancement made in the field of nanotechnology. As far as doping is concerned, transition metals like Fe and Co can be largely utilized and it enhances the physico-chemical properties of the nanoparticles [8]. Moreover, doping of ZnO nanoparticle with transition metals in which the metal site functions as trapping sites by acting as electron acceptors from ZnO there by detaining electron hole recombination and its subsequent reduction in band gap energy. Doping process could be made possible with various methods where sol-gel technique, solid state reaction, co precipitation and pulsed laser decomposition are some of them. Accordingly, doping of transition metals like Fe and Co can complement the antimicrobial properties of ZnO. Certain studies propose that introducing dopants such as Fe and Co into ZnO creates defects in the crystalline lattice. This, in turn, leads to the generation of a higher amount of Reactive Oxygen Species, consequently enhancing antimicrobial activity [9]. Literally cobalt and zinc have similar atomic radii of 0.58 Å and 0.6 Å, respectively. In general doping generally enhances the efficiencies of ZnO in terms of increasing the optical absorption which ultimately reduces the band gap and increases the antimicrobial activity [8].

The present study is focused on exploiting *Alpinia galanga* as a raw material for the green synthesis of ZnO nanoparticles. The aim is to enhance the functionality of the nanoparticles by doping them with Fe and Co to form Fe/ZnO NP and Co/ZnO NP using a co-precipitation method. Furthermore, the pure ZnO and transition metal doped (Fe and Co) ZnO nanoparticles were characterized using FT-IR, EDAX, DLS, UV-Visible spectroscopy, SEM and XRD analysis. Additionally, an antifungal susceptibility test is done by carrying out a well diffusion method against *Candida parapsilopsis*.

## 2. MATERIALS AND METHODS

Healthy leaves of *Alpinia galanga* were collected from kanthalloor region (10.2135°N, 77.1972°E), Idukki District, Kerala, India. *Candida parapsilopsis* culture was obtained from Institute of Microbial Technology Chandigarh, India. Precursors such as Zinc Chloride ( $ZnCl_2$ ), Ferrous Sulphate ( $FeSO_4$ ) and Cobalt Nitrate ( $Co(NO_3)_2$ ) were purchased from Sigma Aldrich.

### 2.1 Methodology

#### 2.1.1. Preparation of plant extract

*Alpinia galanga* leaves were rinsed with purified Milli Q water to remove impurities, dried under shade for 8-10 days, and blend to a fine powder. About 20g of powdered leaf sample were dissolved in 100 ml of Milli Q water and followed by a water bath at 65°C for 25 minutes. Upon cooling the extract was filtered using Whatmann No1 filter paper. The filtrate was used further for the synthesis of ZnO nanoparticles.

#### 2.1.2. Synthesis of ZnO nanoparticles

ZnO nanoparticles were synthesized by gently adding 0.1M zinc chloride solution ( $ZnCl_2$ ) to 25ml of leaf extract in a magnetic stirrer at 60°C for 2 hours [10]. Subsequently, 20ml of 1% NaOH solution was added to the mixture of zinc chloride and leaf extract. When a light yellow coloured precipitate was formed it was allowed to settle for 10 hrs. The particles were separated by centrifugation at 6000 rpm for 20 minutes and were then rinsed three times with distilled water and 70% ethanol to eliminate any traces of impurities. The purified yellow color precipitant was dried overnight at 80°C in hot air oven and powdered to obtain ZnO nanoparticles.

#### 2.1.3. Synthesis of Co doped ZnO and Fe doped ZnO nanoparticles

To synthesize Co-doped ZnO nanoparticles, 1 gram of ZnO nanoparticles was mixed in a conical flask containing 50ml of deionized water (solution A) and stirred continuously for 30 minutes [11,12]. An estimated aliquot of (0.1M) cobalt nitrate solution (solution B) was then added to solution A and stirred further. To this homogeneous mixture, 1g of NaOH and 1% Polyvinylpyrrolidone (PVP) were added. The reaction was proceeded for 2hrs at 5°C to form precipitate of Co doped ZnO nanoparticles. The precipitate was left undisturbed for few hours followed by rinsing with distilled water and 70% ethanol remove any traces of impurities. The purified precipitant was dried overnight in hot air oven at 80°C for 2 days and then powdered.

To synthesize Fe-doped ZnO nanoparticles, 1 gram of ZnO nanoparticles was mixed in a conical

flask containing 50ml of deionized water (solution A) and stirred continuously for 30 minutes [13,14]. An estimated aliquot of (0.1M) ferrous sulfate solution (solution B) was then added to solution A and stirred further. To this homogeneous mixture, 1g of NaOH and 1% PVP were added. The reaction was proceeded for 2hrs at 5°C to form precipitate of Co doped ZnO nanoparticles. The precipitate was left undisturbed for few hours followed by rinsing with distilled water and 70% ethanol remove any traces of impurities. The purified precipitant was dried overnight in hot air oven at 80°C for 2 days and then powdered.

#### 2.2. Characterization of ZnO/Fe doped ZnO/ Co doped ZnO nanoparticles

The crystalline structure and quality of ZnO, Fe doped ZnO and Co doped ZnO NPs were examined using XRD by step scan technique with Cu-K $\alpha$  radiation (1500A°, 40KV, 30 mA) to determine the crystal density [15]. Optical properties of nanoparticles were characterized on the basis of UV-Visible absorption spectra within the wavelength range of 300-700nm [16]. Elemental composition and surface morphology were analyzed using EDAX (Energy Dispersive analysis of X-Ray) and SEM (Scanning electron microscopy model, Hi tech model-s-3400n) [17]. A Perker Elmer 1725X Fourier transform infrared spectrophotometer was used to obtain information about the bond formation in the fabricated nanoparticles. Simultaneously the average size and distribution of nanoparticles were determined by Dynamic Light Scattering analysis [18]

#### 2.3. Antifungal activity of ZnO NPs, Fe doped ZnO NPs and Co doped ZnO NPs

Antifungal activities of ZnO, Fe doped ZnO and Co doped ZnO nanoparticles were performed by agar well diffusion method against *Candida parapsilopsis* [18]. Pure culture of *Candida parapsilopsis* was sub cultured in potato dextrose broth at room temperature in an orbital shaking incubator (Remi, India) at 200rpm. A 100 $\mu$ l of subculture was swabbed on potato dextrose agar plates. Following culture absorption after 10 minutes, wells of 6mm size were punched with the help of a sterile gel puncher. Samples of ZnO, Fe doped ZnO and Co doped ZnO nanoparticles with varying concentrations of 50mg/ml and 100mg/ml were loaded to individually labelled plates. A 10mg/ml concentration of positive control (Amphotericin B) was added to every single well in the plates and a negative control of distilled water was also loaded appropriately using micropipettes. The plates were incubated at room temperature for 48hrs. After 48hrs of incubation, the zone of

inhibition was measured in diameter and the mean values are recorded.

#### 2.4. Determination of Minimum Bactericidal Concentration (MBC), and Minimum Fungicidal Concentration (MFC)

Following a broth dilution method [19] the solutions of nanoparticles (ZnO, Fe doped ZnO and Co doped ZnO) were serially diluted in two folds. A 100 $\mu$ g/ml of sterile PDA broth was added to each well of a 96 well microtitre plates. To the first well, a 100 $\mu$ g/ml concentration of respective nanoparticles was added and mixed uniformly. The suspensions were further transferred and the process continued to obtain a series of dilutions with concentrations of 100, 50, 25, 12.5, and 3.125  $\mu$ g/ml respectively. The wells were further inoculated with 2 $\mu$ l of inoculum and were incubated at room temperature. Further the plates were monitored for turbidity which indicates the presence of growth and non-turbidity indicating the absence of growth. Thus from the experiment the MIC values were investigated. MIC refers to the lowest concentration of nanoparticles which will inhibit the visible growth appearance of microbes after incubating for a required period of time [19,20]. The minimum fungal concentration (MFC) was considered to be the lowest concentration of ZnO, Fe doped ZnO and Co doped ZnO nanoparticles that prevent the development of any single colony of *Candida parapsilopsis* on PDA agar plates following incubation at room temperature.

#### 2.5. Statistical analysis

Every result was shown as mean  $\pm$  standard deviation. Applying SPSS statistical tool, growth attributes were examined at the significant level of  $\leq 0.005$  using T-test to compare the differences between ZnO, Fe doped ZnO, Co doped ZnO, and control, respectively. The possible effects of ZnO, Fe doped ZnO, and Co doped ZnO nanoparticles were evaluated by performing one-way analysis of variance (ANOVA) if P values of  $\leq 0.005$  were proved to be statistically significant.

### 3. RESULTS AND DISCUSSION

#### 3.1. Structural analysis

The structural information of *Alpinia galanga* synthesized ZnO and transition metal doped ZnO (Fe and Co) NPs were analyzed from X-ray diffraction pattern (Fig 1). Figure 1 which shows the XRD spectrum of ZnO, Fe doped ZnO, and Co doped ZnO NPs revealed strong diffraction peaks at 2 $\theta$  value matching to the crystal plane of (100), (002), (101), (102), (110), (103), (112) of respective NPs. In fact, the intense peaks at (100), (101) reveal a crystalline hexagonal wurtzite structure [21].

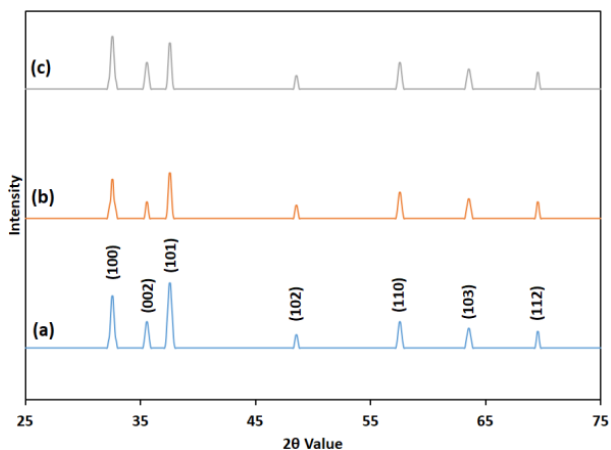


Figure 1. XRD analysis of synthesized nanoparticles (a) ZnO, (b) Co-ZnO and (c) Fe-ZnO  
 Slika 1. XRD analiza sintetizovanih nanočestica (a) ZnO, (b) Co-ZnO i (c) Fe-ZnO

A single phase with no additional peaks (secondary phases) was observed in the Fe, Co, and Fe/Co doped clusters when indexing the peaks with the assistance of the JCPDS-file 36-1451. A similar case was reported by Mohamed et al. [22] in which the fabricated Co/ZnO NPs matched with a standard XRD pattern of ZnO. Hence, XRD pattern add more evidence to the current analysis as it proves the lack of extra peaks in doped ZnO NPs as well as an unaltered hexagonal wurtzite structure in doped ZnO NPs. Therefore all the three NPs have a same XRD spectrum. Elumalai et al. [23] recorded the mean crystalline size (D) of powdered ZnO to be 18nm using Scherrer equation  $D=0.89\lambda/(\beta\cos\theta)$ . Ta et al. [24] reports that there is no significant change in the lattice structure and quality of ZnO crystal upon doping. Hence, the current study reports estimated particle size of 34.64nm, 32nm and 32.19nm for ZnO, Co-ZnO and Fe-ZnO, respectively.

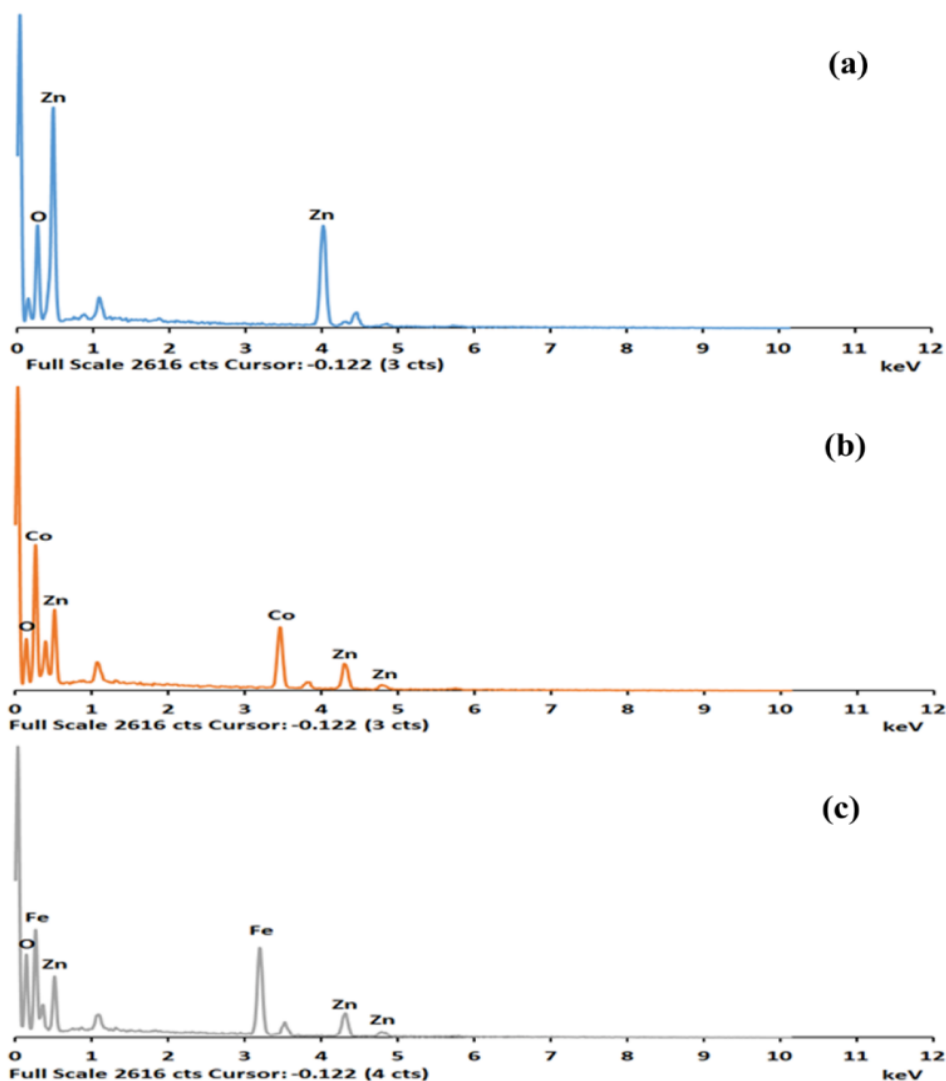


Figure 2. EDX analysis of synthesized nanoparticles (a) ZnO, (b) Co-ZnO and (c) Fe-ZnO  
 Slika 2. EDX analiza sintetizovanih nanočestica (a) ZnO, (b) Co-ZnO i (c) Fe-ZnO

Surface morphology of the ZnO NPs and doped ZnO NPs were investigated using Scanning Electron Microscopy (Fig 2, Fig 3 and Fig 4). Figure recorded under different magnifications reveals that particles are agglomerated with spherical-like and hexagonal-like appearance with a relatively uniform size distribution. Furthermore, the elemental analysis of the synthesized ZnO and doped ZnO NPs was obtained from the corresponding Energy

dispersive X-ray spectrum shown in Fig 5. The accurate elemental composition of NPs in atomic% and weight% recorded are shown in Table 1. A qualitative analysis performed by Sharma et al. [21] confirms the purity of the NPs with the absence of any other foreign materials within the individual spectrum of nanoparticles. This supports the validity of the current study.

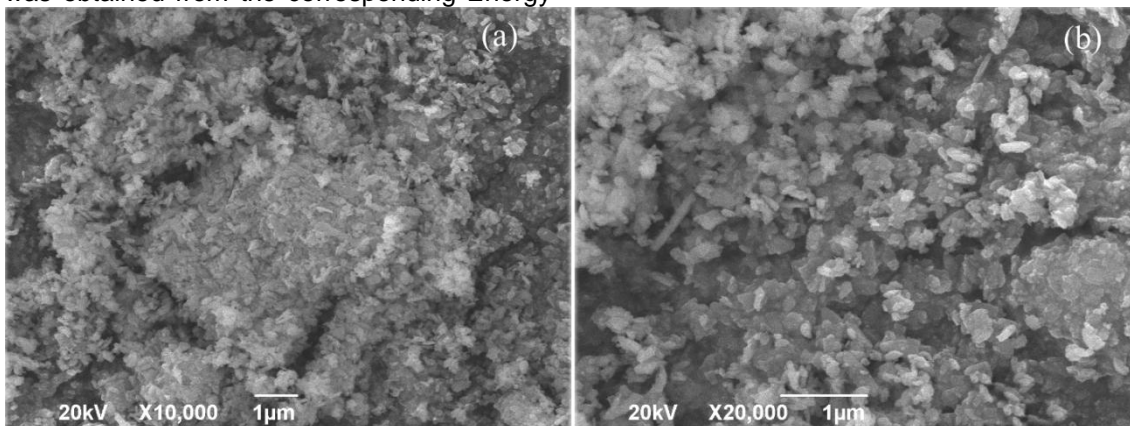


Figure 3. SEM image of *Alpinia galanga* mediated ZnO NPs

Slika 3. SEM slika ZnO NP posredovanih *Alpinia galanga*

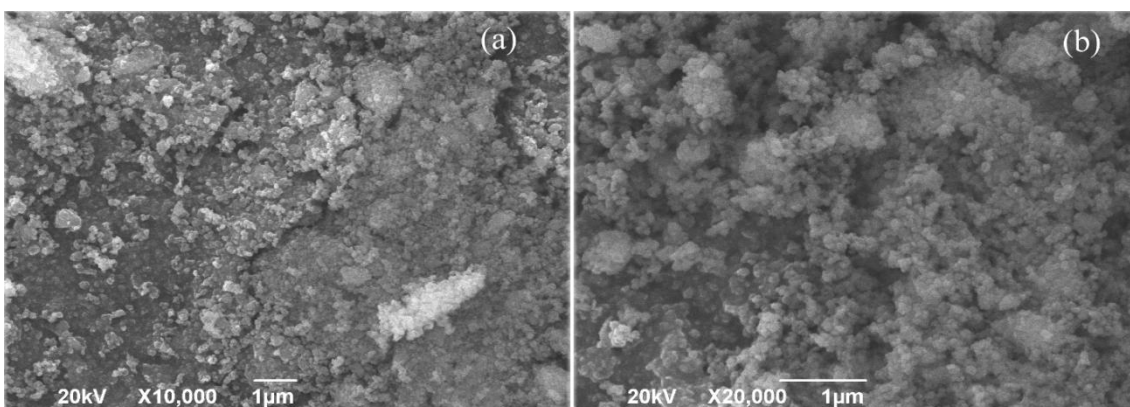


Figure 4. SEM image of Co-ZnO NPs

Slika 4. SEM slika Co-ZnO NP

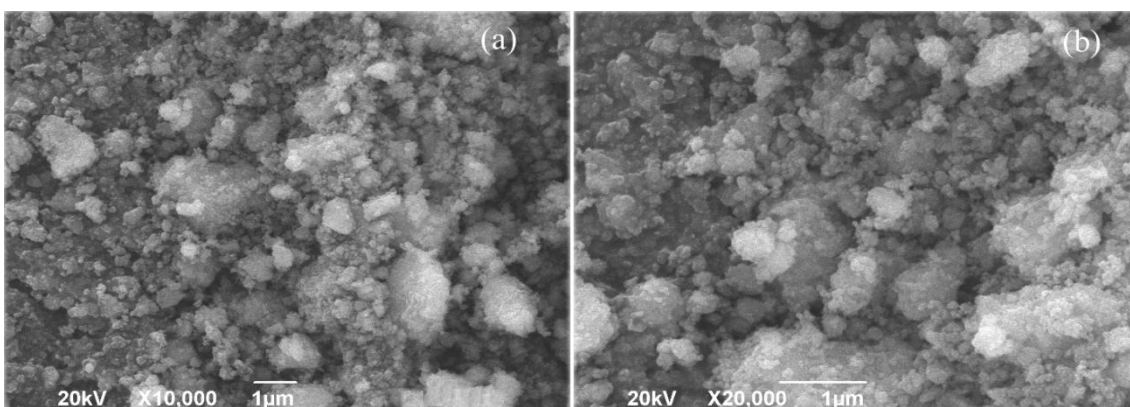


Figure 5. SEM image of Fe-ZnO NPs

Slika 5. SEM slika Fe-ZnO NP

Table 1. EDX analysis of ZnO, Co-ZnO and Fe-ZnO NPs

Tabela 1. EDX analiza ZnO, Co-ZnO i Fe-ZnO NP

Elements	Atomic percentage (%)				Weight percentage (%)			
	Zn	Co	Fe	O	Zn	Co	Fe	O
ZnO	36.71	-	-	63.29	69.73	-	-	30.27
Co-ZnO	11.28	13.91	-	74.81	26.78	29.76	-	43.46
Fe-ZnO	11.49	-	20.37	68.15	25.21	-	38.19	36.61

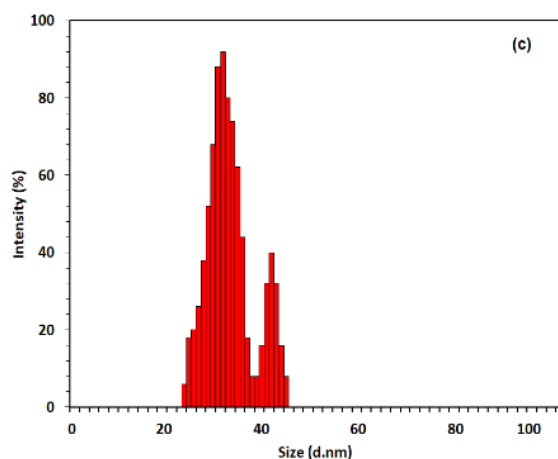
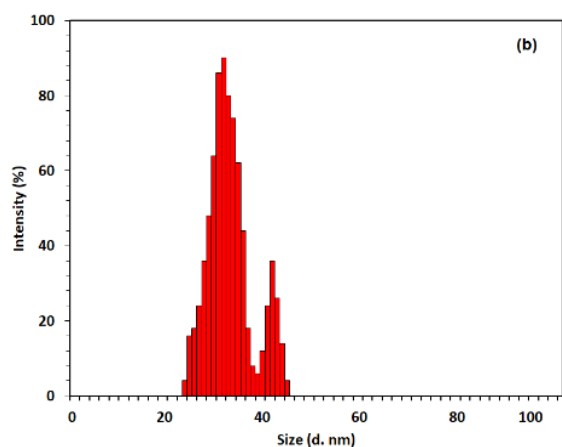
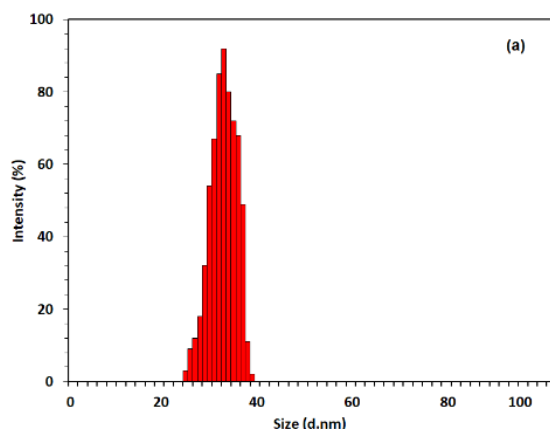


Figure 6. Particle size analysis of (a) ZnO, (b) Co-ZnO and (c) Fe-ZnO NPs

Slika 6. Analiza veličine čestica (a) ZnO, (b) Co-ZnO i (c) Fe-ZnO NP

### 3.3. Particle size analysis

Dynamic Light Scattering studies is used to determine the average size distribution profile of the ZnO, Fe doped ZnO and Co doped ZnO nanoparticles (Fig 6).

Table 2 shows the average size distribution of the NPs and which confirm the results obtained by XRD and SEM. The average size (Z) of ZnO, Co-ZnO and Fe-ZnO was found to be 36, 32 and 32 nm, respectively.

Table 2. The average size distribution of ZnO, Co-ZnO and Fe-ZnO NPs estimated by using Particle size analysis

Tabela 2. Prosečna distribucija veličine ZnO, Co-ZnO i Fe-ZnO NP procenjena korišćenjem analize veličine čestica

Nanoparticles	Size distribution (d.nm)	Z- Average size (d.nm)
ZnO	24-38	36
Co-ZnO	22-44	32
Fe-ZnO	22-44	32

### 3.4. Fourier Transform Infrared spectroscopy (FTIR)

The characteristic major peaks in the FTIR spectrum of *A. galanga* leaf extract show a broad band at  $3143\text{ cm}^{-1}$  and  $3444\text{ cm}^{-1}$  due to O-H stretching and bending vibrations of polyphenols (Fig 7 and Table 3). A slender band at  $1768\text{ cm}^{-1}$  reveals the C=O stretch corresponding to carboxylic acid. Similarly, the peak at  $1056\text{ cm}^{-1}$  is attributed to an O-H bend. Intense sharp bands at  $1400\text{ cm}^{-1}$  and  $1637\text{ cm}^{-1}$  correspond to aromatic (C=C stretch) functional groups [17]. The band at  $1637\text{ cm}^{-1}$  represents the N-H bending vibrations of primary amines. Moreover, the bands at  $619\text{ cm}^{-1}$  correspond to bending vibrations of alkynes (=C-H) and stretching vibrations of alkyl halides respectively.

FTIR spectrum revealed the function of phytochemicals as a capping agent during the synthesis of ZnO NPs. When the bioactive compound is bound to the surface of ZnO NPs it subsequently results in the reduction and stabilization of NPs (phenolic compounds, amines, ether, carboxylic acids, and hydroxyl groups) [18].

For the reduction of  $Zn^{2+}$  to  $Zn^0$  O-H, C-N and N-H groups are involved [17]. Furthermore, ZnO/Co-ZnO/Fe-ZnO NPs spectrum exhibit a similar broad absorption band at  $3142\text{ cm}^{-1}$ ,  $3379\text{ cm}^{-1}$ ,  $3140\text{ cm}^{-1}$  [18] corresponding to stretching vibration H bending vibrations in alcohol (Fig 8 and Table 4). The band at  $3140\text{ cm}^{-1}$  in Co doped ZnO NP corresponds to H bending vibrations. Similarly, an intense band at  $1402\text{ cm}^{-1}$  and  $1400\text{ cm}^{-1}$  corresponds to C=C stretch in aromatic ring. There is an absence of C=O stretching vibrations in

synthesized ZnO, Co-ZnO, Fe-ZnO spectrums. Vijayakumar et al. [18] reported that the peaks from  $700\text{--}900\text{ cm}^{-1}$  in FTIR spectra of ZnO particles are attributed to the bond formation between Fe and O, confirming the synthesis of Fe-doped ZnO nanoparticles. Similarly Sharma et al. [21] also confirmed the presence of a band at  $875\text{ cm}^{-1}$  which was referred as the frequency of metal oxide vibrations due to the changes in the features of metal resulting from doping of cobalt metal oxide precursor.

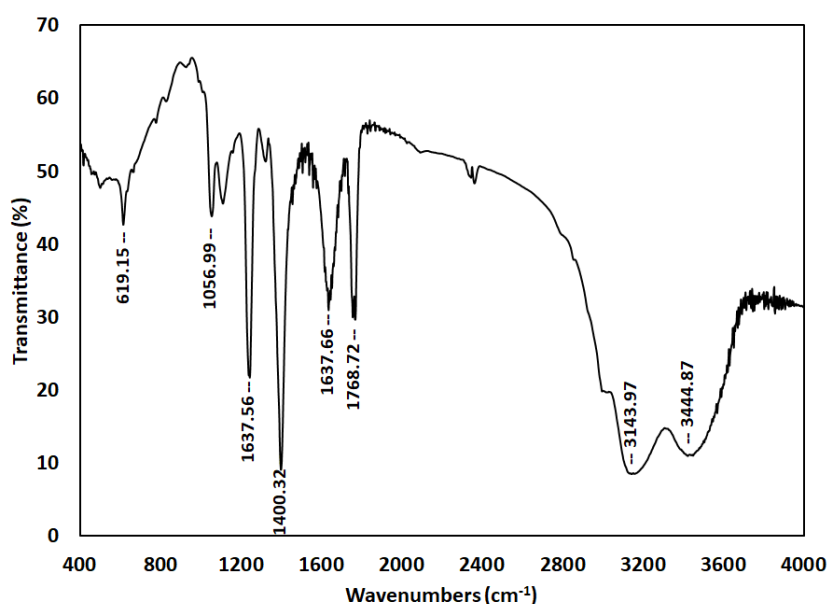


Figure 7. FTIR analysis of *Alpinia galangal* aqueous extract

Slika 7. FTIR analiza vodenog ekstrakta *Alpinia galangal*

Table 3. FTIR analysis of ZnO, Co-ZnO and Fe-ZnO NPs

Tabela 3. FTIR analiza ZnO, Co-ZnO i Fe-ZnO NP

Functional group and bond		<i>A. galanga</i>	ZnO	Co:ZnO	Fe:ZnO
Alkynes	=C-H (Bending)	619.15	617.22	688.59	617.22
Alkyl halides	C-Cl stretch		-	-	831.32
carboxylic acids	O-H bend	1056.99	-	941.26	-
Primary amines	N-H bend	1637.56	1639.49	1624.06	1639.49
Amine	C-N (Stretch)		1128.36	1128.36	1130.29
Aromatic	C=C (Stretch)	1400.32, 1637.66	1402.25	1402.25	1400.32
Carboxylic acid	C=O stretch	1768.72	-	-	-
Alcohol	O-H (Stretch, H-bending)	3143.97, 3444.87	3142.04	3379.29, 3140.11	3140.11

### 3.5. Antifungal Assay

Antifungal assay of ZnO, Co doped ZnO and Fe doped ZnO NPs against *Candida parapsilopsis* was determined by the well diffusion method. Table 4 shows the details of resulting zone of inhibition

against standard Amphotericin B (AmB). A concentration dependent antifungal activity is observed from these results. An ANOVA test clarifies that the results obtained were statistically significant.

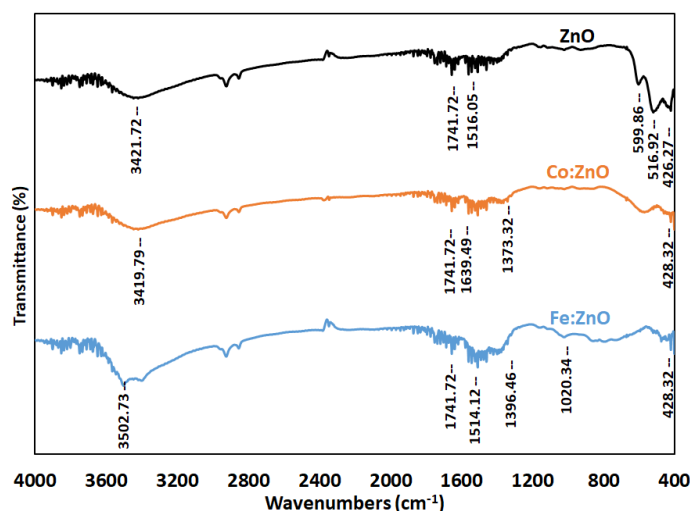


Figure 8. FTIR analysis of ZnO, Co-ZnO and Fe-ZnO NPs

Slika 8. FTIR analiza ZnO, Co-ZnO i Fe-ZnO NPs

Table 4. Antifungal activity of ZnO, Co-ZnO and Fe-ZnO NPs against candida parasilopsis. The resulted zone of inhibition (mm) are expressed in Mean ± SD

Tabela 4. Antifungalna aktivnost ZnO, Co-ZnO i Fe-ZnO NP protiv candida parasilopsis. Dobjena zona inhibicije (mm) je izražena kao srednja vrednost ± SD

Nanoparticles	Different concentration of Nanoparticles		Control (Amphotericin B 10 mg/ml)	Mean ± SD	t test	F	Sig.
	50 mg/L	100 mg/L					
ZnO	8.66 ± 0.57	9.50 ± 0.50		8.27 ± 1.34	11.738	20.818	0.002*
Co-ZnO	8.33 ± 0.57	9.00 ± 1.00	5.77 ± 0.57	7.77 ± 1.56	9.168	17.357	0.006*
Fe-ZnO	8.66 ± 0.57	12.00 ± 1.00		8.88 ± 1.71	6.512	34.857	0.000*

Figure 9 shows the zone of inhibition of ZnO/Co-ZnO/Fe-ZnO at 50 and 100mg/L. The highest zone of inhibition against *Candida parasilopsis* observed had with a diameter of 9.50±0.50 at a concentration of 100mg/L (Fig 9). Likewise zone of inhibition is 9.00±1.00 and 12.00±1.00 for Co-ZnO and Fe-ZnO NPs, respectively. The observed zone of inhibition against *Candida parasilopsis* is specified for ZnO/Co-ZnO/Fe-ZnO at concentrations of 50 and 100mg/L. The data shows the highest zone of inhibition (with a diameter of 9.50±0.50) at a concentration of 100mg/L. Additionally, specific values for the zone of inhibition are provided for

Co-ZnO and Fe-ZnO NPs. The concluding statement ties these results together by attributing the increased antifungal activity to the synergistic effect of doping in the nanoparticles. The supporting evidence comes from the observed zone of inhibition values for different nanoparticle formulations at varying concentrations. Additionally, the present analysis supports the fact that particles in nano dimensions have effective properties compared to their macro dimensions. Upon comparing the zones of clearance observed around both the standard and samples, it was found that all three types of nanoparticles were effective in inhibiting growth [23].

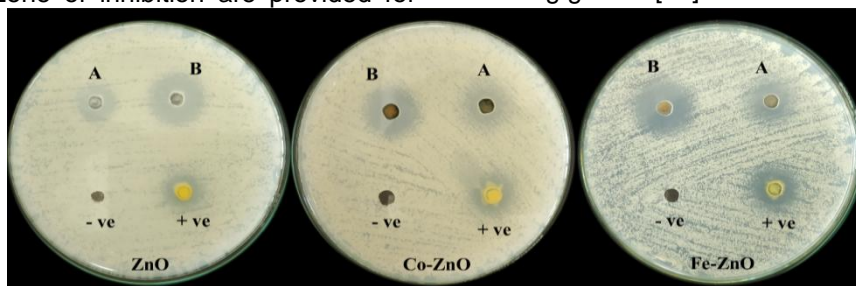


Figure 9. Antifungal activity of ZnO, Co-ZnO and Fe-ZnO NPs on candida parasilopsis

Slika 9. Antifungalna aktivnost ZnO, Co-ZnO i Fe-ZnO NP na candida parasilopsis

The MIC and MFC values of synthesized ZnO, Fe doped ZnO and Co doped ZnO NPs are shown (Table 5). From these values, The MIC for ZnO NPs is observed at a concentration of 12.5 $\mu\text{g/ml}$ , while both Co-ZnO and Fe-ZnO NPs share identical MIC values at a concentration of 3.125 $\mu\text{g/ml}$ . The MFC values show significant value of 25 $\mu\text{g/ml}$  for ZnO NPs, 3.125 $\mu\text{g/ml}$  for Fe-ZnO and Co-ZnO NPs. Thus evaluating MIC and MFC, a potential MIC/MFC ratio was calculated to be 2;1;1 for ZnO; Fe-ZnO; Co-ZnO NPs.

Table 5. MIC ( $\mu\text{g/ml}$ ) and MBC ( $\mu\text{g/ml}$ ) values of ZnO, Co-ZnO and Fe-ZnO NPs against *Candida parasilopsis*

Tabela 5. MIC ( $\mu\text{g/ml}$ ) i MBC ( $\mu\text{g/ml}$ ) vrednosti ZnO, Co-ZnO i Fe-ZnO NP protiv *parasilopsis kandide*

Nanoparticles	MIC ( $\mu\text{g/ml}$ )	MBC ( $\mu\text{g/ml}$ )	MBC/MIC ratio
ZnO	12.5	25	2
Co-ZnO	3.125	3.125	1
Fe-ZnO	3.125	3.125	1

The biofilm inhibitory activity of synthesized nanoparticles was determined by a standard crystal violet method performed on micro titration plates. Figures 10 reveal the light microscopic observation of the biofilm and the image recorded using an inverted microscope under 40X magnification (Fig 11). Figure 10 shows the effective inhibition of fungal hyphae according to standard 10mg AmB and 100mg, 50mg, and 25mg of Fe-ZnO. The figure10 shows a synergistic effect in the biofilm inhibitory activity by Fe-ZnO compared to that Co-ZnO in the same concentration range. Nevertheless, the rest of the concentrations also exhibit an appreciating inhibitory activity against a pathogenic *Candida parapsilopsis* biofilm. Eventually, there is a decreased aggregation of planktonic cells in the biofilm compared to control (absence of nanomaterial). In the case of both light and inverted microscopic observations both the nanoparticles appeared to have a concentration dependent anti biofilm activity against the *Candida parapsilopsis* strain.

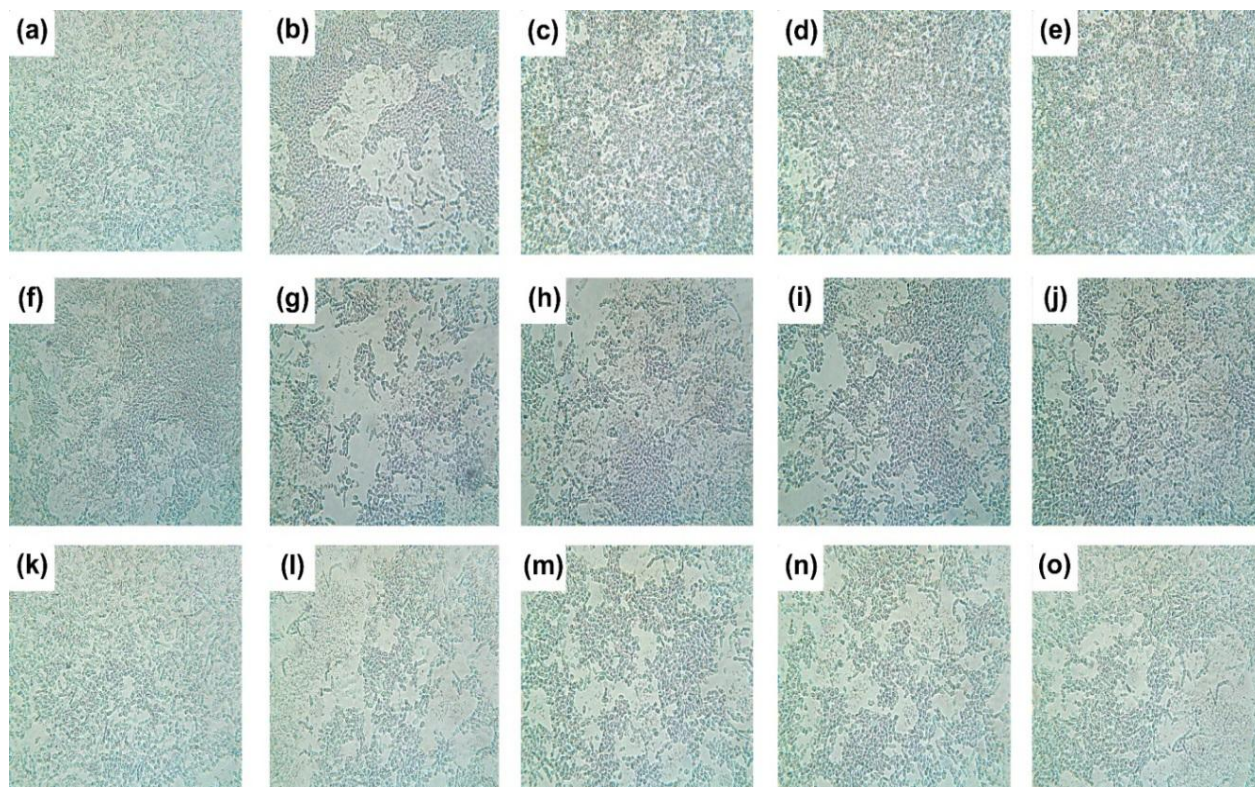


Figure 10. CV stained light microscopic observation of the biofilm inhibitory assay of ZnO (a-e), Co-ZnO (f-j) and Fe-ZnO (k-o) NPs on *C.parasilopsis*

Slika 10. CV obojeno svetlosnim mikroskopskim posmatranjem testa inhibitora biofilma ZnO (a-e), Co-ZnO (f-j) i Fe-ZnO (k-o) NP na *C.parasilopsis*

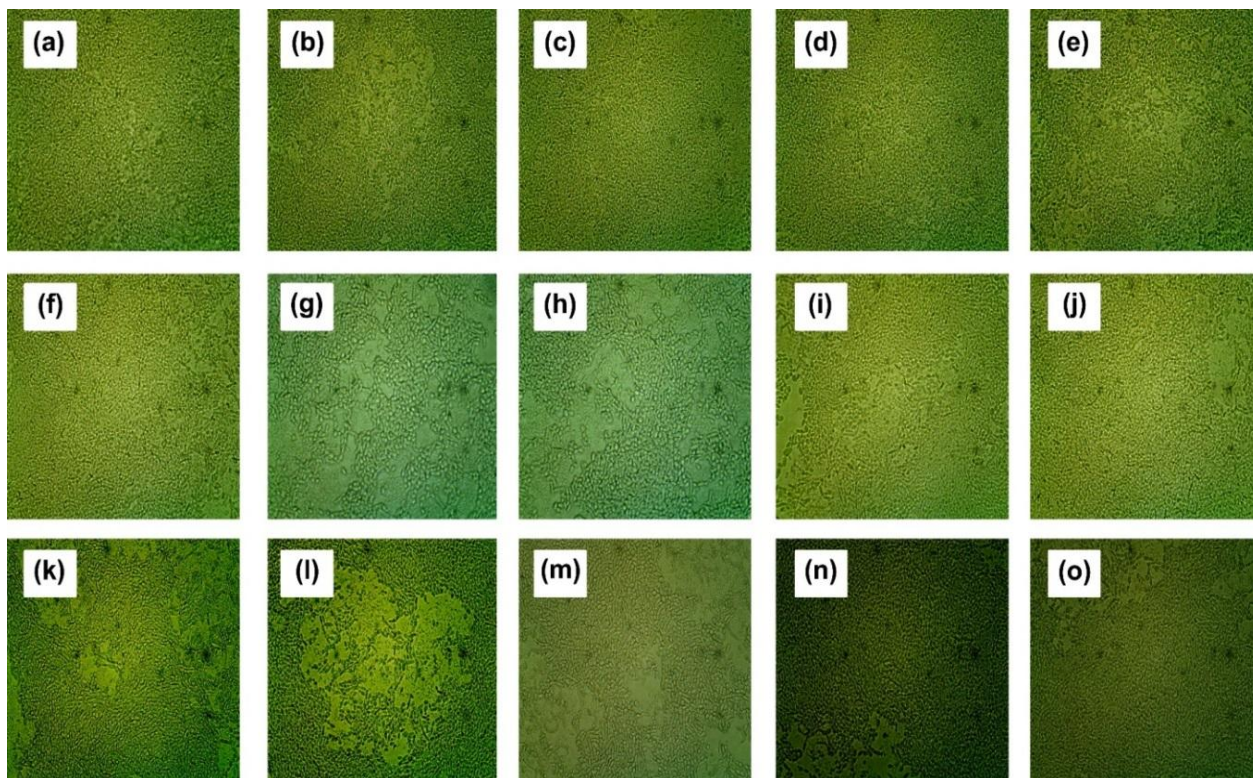


Figure 11. The image obtained from inverted microscope under 40X magnification for of ZnO (a-e), Co-ZnO (f-j) and Fe-ZnO (k-o) NPs

Slika 11. Slika dobijena invertovanim mikroskopom pod uvećanjem od 40Ks za ZnO (a-e), Co-ZnO (f-j) i Fe-ZnO (k-o) NPs

#### 4. CONCLUSION

The present study was carried out on the synergistic effect of Fe and Co doped ZnO nanoparticles synthesized using *Alpinia galanga* leaf extract and their in vitro antifungal activity. ZnO NPs were successfully synthesized and doped with transition metal precursors to generate Fe doped ZnO and Co doped ZnO NPs by co precipitation method. The nanoparticles fabricated under optimized process conditions were characterized using FTIR, XRD, SEM, DLS, EDAX and the results were evaluated. In vitro antifungal susceptibility tests revealed the fascinating antifungal efficiencies of three NPs against *Candida parapsilopsis* when compared to a standard Amphotericin B. Hence, these nanoparticles could be largely exploited for biomedical applications. Moreover, it strongly emphasizes the need to execute a green synthesis approach for synthesizing metallic/metal oxide nanoparticles rather than a chemical approach. This particular work is regarded as an environmentally safe, inexpensive method and the process could be effectively practiced on large scales. The nanoparticles can be explored as a novel nano therapeutic medicine in future.

#### Acknowledgment

We thank to the Management of Sri Krishna Arts and Science College, Coimbatore, Tamil Nadu, India for the Seed money grant and providing necessary facilities to carry out this work.

#### 5. REFERENCES

- [1] E.J. Baron, J.M. Miller (2008) Bacterial and fungal infections among diagnostic laboratory workers: evaluating the risks. *Diagn. Micr. Infec. Dis.*, 60(3), 241–246, <https://doi.org/10.1016/j.diagmicrobio.2007.09.016>
- [2] J. Kaur, C.J. Nobile (2023) Antifungal drug-resistance mechanisms in *Candida* biofilms. *Curr. Opin. Microbiol.*, 71, 102237, <https://doi.org/10.1016/j.mib.2022.102237>
- [3] A. Espinel-Ingroff (2009) Novel antifungal agents, targets or therapeutic strategies for the treatment of invasive fungal diseases: a review of the literature (2005-2009). *Rev. Iberoam. Micol.*, 26(1), 15–22, [https://doi.org/10.1016/s1130-1406\(09\)70004-x](https://doi.org/10.1016/s1130-1406(09)70004-x)
- [4] A. Chaturvedi, S. Shambhakar (2024) Nanotechnology in Drug Delivery: Overcoming Poor Solubility Challenges through Nanoformulations. *Nanomed. J.*, 14, In Press, <https://doi.org/10.2174/0124681873276732231207051324>

- [5] T.A.Wani, G.Suresh (2022) Plant-Mediated Green Synthesis of Magnetic Spinel Ferrite Nanoparticles: A Sustainable Trend in Nanotechnology. *Adv. Sustain. Syst.*, 6(6), <https://doi.org/10.1002/adsu.202200035>
- [6] A.Burhan, D.Ratnadewi, A.Setiyono, R.Astuti, A. Umar (2024) Phytochemical Profiling of Hippobroma longiflora Leaf Extract Using LC-MS/MS Analysis and Pharmacological Potential. *Egypt. J. Chem.*, 23, <https://doi.org/10.21608/ejchem.2024.242541.8740>
- [7] S.Chandrasekaran, V.Anbazhagan (2023) Green Synthesis of ZnO and V-Doped ZnO Nanoparticles Using Vinca rosea Plant Leaf for Biomedical Applications. *Appl. Biochem. Biotechnol.*, 196(1), 50–67. <https://doi.org/10.1007/s12010-023-04546-2>
- [8] M.Duan, J.G.Shapter, W.Qi, S.Yang, G.Gao (2018) Recent progress in magnetic nanoparticles: synthesis, properties, and applications. *Nanotechnol.*, 29(45), 452001, <https://doi.org/10.1088/1361-6528/aaadcec>
- [9] M.S.Nadeem, T.Munawar, F.Mukhtar, M.Naveed, U. Rahman, M.Riaz, F.Iqbal (2021) Enhancement in the photocatalytic and antimicrobial properties of ZnO nanoparticles by structural variations and energy bandgap tuning through Fe and Co co-doping. *Ceram. Int.*, 47(8), 11109–11121, <https://doi.org/10.1016/j.ceramint.2020.12.234>
- [10] R.R.Muthu Chudarkodi, A.Rajalaxshmi (2016) Synthesis, Electrochemical Characterization and Photocatalytic Application of Ceion Doped ZnO nanoparticles using Leaf Extract of SesbaniaGrandiflora by Green Method. *Int. J. Sci. Res.*, 5(3), 1073–1080. <https://doi.org/10.21275/v5i3.15031601>
- [11] S.Chandrasekaran, V.Anbazhagan (2023) Green Synthesis of ZnO and V-Doped ZnO Nanoparticles Using Vinca rosea Plant Leaf for Biomedical Applications. *Appl. Biochem. Biotechnol.*, 196(1), 50–67. <https://doi.org/10.1007/s12010-023-04546-2>
- [12] D.Giram, A.Das (2024) Synthesis and characterization of Fe doped ZnO nanoparticles for the photocatalytic degradation of Eriochrome Black-T dye. *Indian J. Chem. Techn.*, In press, <https://doi.org/10.56042/ijct.v31i1.4985>
- [13] D.Gupta, R.K.Ghanshyam Kotnala, N.S.Negi (2013) Synthesis and characterization of Cu, Fe co-doped ZnO nano-particles synthesized by solution combustion method. *AIP Conference Proceedings*. <https://doi.org/10.1063/1.4810156>
- [14] P.Dhiman, R.Rani, M.Singh (2012) Structural and electrical properties of Fe doped ZnO nanoparticles synthesized by solution combustion method. *AIP Conference Proceedings*. <https://doi.org/10.1063/1.4710002>
- [15] P.Dhiman, J.Chand, S.Verma Sarveena, M.Singh (2014) Ni, Fe Co-doped ZnO nanoparticles synthesized by solution combustion method. *AIP Conference Proceedings*. <https://doi.org/10.1063/1.4872990>
- [16] N.Madkhali (2022) Analysis of Structural, Optical, and Magnetic Properties of (Fe,Co) Co-Doped ZnO Nanoparticles Synthesized under UV Light. *Condens. Matter.*, 7(4), 63-71, <https://doi.org/10.3390/condmat7040063>
- [17] P.Malathy, S.Selvarajan (2018) Visible Light Assisted Photocatalytic Activity of Co-doped ZnO, In-Doped ZnO and (Co, In) co- doped ZnO Nanoparticles. *Int. J. Nanotechnol. App.*, 8(1), 1–14, <https://doi.org/10.24247/ijnajun20181>
- [18] T.S.Boopathi, S.Suksom, J.Suriyaprakash, A.H. Hirad, A.A.Alarfaj, I.Thangavelu (2024) Psidium guajava-mediated green synthesis of Fe-doped ZnO and Co-doped ZnO nanoparticles: a comprehensive study on characterization and biological applications. *Biopro. Biosyst. Eng.*, in press, <https://doi.org/10.1007/s00449-024-03002-7>
- [19] W.Kejela Tolossa, P.Taddesse Shibeshi (2022) Structural, optical and enhanced antibacterial activities of ZnO and (Co, Fe) co-doped ZnO nanoparticles by sol-gel combustion method. *Chem. Phys. Lett.*, 795, 139519, <https://doi.org/10.1016/j.cplett.2022.139519>
- [20] I.O.Chikezie (2017) Determination of minimum inhibitory concentration (MIC) and minimum bactericidal concentration (MBC) using a novel dilution tube method. *Afr. J. Microbiol. Res.*, 11(23), 977–980, <https://doi.org/10.5897/ajmr2017.8545>
- [21] D.Sharma, R.Jha (2017) Transition metal (Co, Mn) co-doped ZnO nanoparticles: Effect on structural and optical properties. *J. Alloys Compd.*, 698, 532–538, <https://doi.org/10.1016/j.jallcom.2016.12.227>
- [22] M.Ram, K.Bala, H.Sharma, A.Kumar, N.S.Negi (2016) Investigation on structural and electrical properties of Fe doped ZnO nanoparticles synthesized by solution combustion method. *AIP Conference Proceedings*. <https://doi.org/10.1063/1.4946078>
- [23] M.D.Sahadat Hossain, S.Ahmed (2023) Easy and green synthesis of TiO<sub>2</sub> (Anatase and Rutile): Estimation of crystallite size using Scherrer equation, Williamson-Hall plot, Monshi-Scherrer Model, size-strain plot, Halder- Wagner Model. *Results Mater.*, 20, 100492, <https://doi.org/10.1016/j.rinma.2023.100492>
- [24] X.Han, S.Wahl, P.Russo, N.Pinna (2018) Cobalt-Assisted Morphology and Assembly Control of Co-Doped ZnO Nanoparticles. *Nanomater.*, 8(4), 249, <https://doi.org/10.3390/nano8040249>
- [25] M.Mittal, M.Sharma, O.P.Pandey (2014) UV-Visible light induced photocatalytic studies of Cu doped ZnO nanoparticles prepared by co-precipitation method. *J. Sol. Energy.*, 110, 386–397, <https://doi.org/10.1016/j.solener.2014.09.026>
- [26] D.Sharma, R.Jha (2017) Analysis of structural, optical and magnetic properties of Fe/Co co-doped ZnO nanocrystals. *Ceram. Int.*, 43(11), 8488–8496, <https://doi.org/10.1016/j.ceramint.2017.03.201>
- [27] Y.Köseoğlu (2015) Rapid synthesis of room temperature ferromagnetic Fe and Co co-doped ZnO DMS nanoparticles. *Ceram. Int.*, 41(9), 11655–11661, <https://doi.org/10.1016/j.ceramint.2015.05.127>

## IZVOD

### **SINERGISTIČKI EFEKAT NANOČESTICA ZnO DOPIRANIH Fe I Co SINTETIZOVANIH KORIŠĆENJEM *ALPINIA GALANGA* PROTIV *CANDIDA PARASILOPSIS***

*U ovom istraživanju, nanočestice kao što su ZnO, ZnO dopiran Fe i ZnO NP dopiran Co pripremljene metodom koprecipitacije su testirane protiv patogenog kvasca. Spektroskopske analize su sprovedene radi identifikacije morfološkog i hemijskog sastava sintetizovanih nanočestica. Rezultati XRD analize su otkrili da su sintetizovane nanočestice kristalne prirode sa prosečnim rasponom veličine između 32 – 34 nm približno. EDKS i SEM analize su sprovedene da bi se identifikovao sastav elemenata (Co, Fe i Zn) i sferni oblik nanočestica. Funkcionalna grupa koja je odgovorna za zatvaranje i stabilnost nanočestica je potvrđena FTIR analizom, da bi se uporedila antifungalna efikasnost ZnO, ZnO dopiranog Fe i ZnO dopiranog Co iz rezultujuće zone inhibicije.*

**Ključne reči:** *Antifungalna aktivnost, Candida parapsilosis, bakar, gvožđe, cink*

*Naučni rad*

*Rad primljen: 27. 09. 2023.*

*Rad prihvaćen: 09. 12. 2023.*

*Rad je dostupan na sajtu: [www.idk.org.rs/casopis](http://www.idk.org.rs/casopis)*